0026-895X/96/060949-07$3.00/0

MOLECULAR PHARMACOLOGY, 49:949–955 (1996).

ACCELERATED COMMUNICATION

High Affinity Open Channel Block by Dofetilide of *HERG* Expressed in a Human Cell Line

DIRK J. SNYDERS and ARCHANA CHAUDHARY

Departments of Medicine (D.J.S.) and Pharmacology (D.J.S., A.C.), Vanderbilt University School of Medicine, Nashville, Tennessee 37232-6602

Received November 10, 1995; Accepted February 26, 1996

SUMMARY

In the long QT syndrome, excessive prolongation of the cardiac action potential leads to polymorphic ventricular tachycardia (torsades de pointes) and sudden death. Mutations in *HERG* have been identified as one of the causes of the chromosome 7-linked form of congenital long QT syndrome. The biophysical properties of currents recorded from *HERG* expressing *Xenopus* oocytes are similar to those of a cardiac K^+ current, I_{Kr}, but the characteristic nanomolar methanesulfonanilide sensitivity has not been demonstrated. To determine the biophysical and pharmacological properties of *HERG* under experimental conditions similar to those used to study native cardiac currents, we examined currents expressed after expression of *HERG* in a human cell line, human embryonic kidney 293. Transfected cells displayed K^+-selective outward currents that activated at membrane potentials positive to −50 mV with strongly voltage-dependent kinetics [time constant (τ) = 2 sec at −20 mV and 188 msec at +20 mV]. Marked inward rectification was observed for depolarizations positive to +0 mV, which was due to rapid channel inactivation (τ = 6 msec at +50 mV). The subsequent tail currents at −40 mV displayed an initial rising phase with τ = 10 msec, followed by a slow multiexponential decline. The EC_{50} for the methanesulfonanilide I_{Kr} blocker dofetilide was 12 ± 2 nM. Induction of block depended on depolarization beyond the threshold for channel opening. Time-dependent block developed slowly, with τ = 5.2 ± 0.6 sec (300 nM) at +10 mV, and was delayed by stronger depolarizations. This pattern suggested that dofetilide preferentially blocks open (or activated) channels and that the fast inactivation may competitively slow the binding kinetics. The latter occurrence was further supported by a simplified mathematical model that addressed the impact on binding kinetics of fast inactivation. These results indicate that the *HERG* gene product encodes an α subunit that, when expressed in mammalian cells, displays both the major functional and pharmacological properties of native I_{Kr}. Dofetilide acts as a slow-onset/slow-offset open channel blocker of this current at nanomolar concentrations.

I_{Kr} plays an important role in controlling cardiac action potential duration and displays several characteristics: inward rectification, sensitivity to micromolar lanthanum, and specific nanomolar block by the methanesulfonanilide class of antiarrhythmic agents (e.g., E4031, dofetilide, almokalant) (1-8). Block of repolarizing potassium currents not only results in action potential prolongation as an antiarrhythmic intervention but also can be associated with a proarrhythmic side effect: acquired LQTS (9), and the polymorphic ventricular arrhythmia torsades de pointes (10). Mutations in *HERG* (11) have recently been identified in patients with the chromosome 7-linked form of congenital LQTS (12). Functional expression of the wild-type gene product in *Xenopus* oocytes revealed that *HERG* encodes a potassium current with biophysical properties similar to those of I_{Kr} in cardiac myocytes: an outward current that displays inward rectification at positive potentials and large, slowly deactivating tail currents at more negative voltages (13). Another report showed large inward currents that are more similar to typical inward rectifier currents but have a slower time-dependent component (14). *HERG* was reported to be insensitive to the methanesulfonanilide blockers (13), which was unexpected because these drugs are thought to specifically target I_{Kr} in myocytes of various species, including human (15). Trudeau *et al.* (14) found that high concentrations of E4031 did block *HERG* expressed in oocytes (EC_{50} ~ 600 nM); the latter is ~20-fold higher than the EC_{50} found for action potential prolongation or I_{Kr} block (16, 17). This raises the

This work was supported by National Institutes of Health Grants HL47599 and HL46681 and a Grant-in-Aid from the American Heart Association.

ABBREVIATIONS: LQTS, long QT syndrome; *HERG*, human *ether-a-gogo*-related gene; HEPES, 4-(2-hydroxylethyl)-1-piperazineethanesulfonic acid; GFP, green fluorescent protein; HEK, human embryonic kidney; I_{Kr}, rapidly activating delayed rectifier K^+ current.

possibility that expression in oocytes might modify the pharmacology for these blockers. Alternatively, the molecular architecture of the native channel might involve an accessory subunit that would endow *HERG* with the proper pharmacology (13). To test whether the *HERG* cDNA that did not display typical I_{Kr} currents in oocytes (14) is capable of generating inwardly rectifying outward current with the proper pharmacology, we expressed this gene product in human cells. After demonstrating functional I_{Kr}-like currents, we determined the mechanism of dofetilide block under conditions similar to those used for cardiac myocytes but with the advantage of minimal contamination from overlapping ionic conductances.

Materials and Methods

Transfection and cell culture. Recently thawed human HEK 293 cells (American Type Culture Collection No. 1573-CRL, passage 33) were maintained in Eagle's minimum essential medium supplemented with 10% horse serum. The cells were transfected through the lipofectamine method according to the manufacturer's instructions (GIBCO-BRL). The *HERG* clone in the pBK_{CMV} expression vector (which contains three point mutations, E91D, V198E, and P202L, compared with the published *HERG* sequence) was kindly provided by Dr. G. Robertson (University of Wisconsin, Madison, WI). GFP (18) was coexpressed to allow assessment of the transfection efficiency and identification of cells for voltage-clamp analysis. We applied a mixture of 1-3 μg of *HERG*/pBK_{CMV}, 4 μg of GFP/pRC_{CMV}, and 25 μl of lipofectamine reagent for 6 hr, after which the standard medium was restored. The cells were removed from the dish 48 hr later with the use of brief trypsinization, washed twice in standard media, and stored for use within the next 12 hr. Parallel nontransfected cultures or cells transfected with GFP only (mock transfection) served as controls.

Electrical recording. Recordings were made with a DAGAN 3900 patch-clamp amplifier (Dagan Corp., Minneapolis, MN) using the whole-cell configuration of the patch-clamp technique (19). Cells were allowed to settle to the bottom of a small perfusion chamber (0.5 ml) mounted on the stage of a Nikon Diaphot 200 microscope. The latter was equipped for epifluorescence with a B2A filter assembly to observe the GFP fluorescence of successfully transfected cells. Currents were recorded at room temperature (21-23°) and sampled at 0.2-10 kHz after antialias filtering at half the sampling frequency. Data acquisition and command potentials were controlled with the use of pClamp software (Axon Instruments, Foster City, CA). Micropipettes were pulled from starbore borosilicate glass (Radnoti) and heat polished. The average pipette resistance was 2.4 ± 0.1 MΩ (21 experiments). Junction potentials were zeroed with the pipette in the standard bath solution. Gigaohm seal formation was achieved through the use of suction (13 ± 2 GΩ; range, 8-27 GΩ). After establishment of the whole-cell configuration, the capacitive transients elicited by symmetrical 10-mV voltage-clamp steps from −80 mV were recorded at 50 kHz (filtered at 10 kHz) for calculation of capacitive surface area and access resistance, which were 13.9 ± 0.9 pF and 4.9 ± 0.3 MΩ, respectively. After compensation, the residual access resistance was 0.8 ± 0.2 MΩ, resulting in voltage errors of <1 mV because the recorded currents did not exceed 1 nA.

Solutions and chemicals. The intracellular pipette filling solution contained 110 mM KCl, 10 mM HEPES, 5 mM K_2-ATP, 5 mM K_4-1,2-bis(2-aminophenoxy)ethane-*N*′,*N*′,*N*′,*N*′-tetraacetic acid, and 1 mM $MgCl_2$, adjusted to pH 7.2 with KOH to yield a final intracellular K^+ concentration of ~145 mM. The bath solution contained 130 mM NaCl, 4 mM KCl, 1.8 mM $CaCl_2$, 1 mM $MgCl_2$, 10 mM HEPES, and 10 mM glucose, adjusted to pH 7.35 with NaOH. Dofetilide was provided by Pfizer Central Research. All other chemical compounds were obtained from Sigma Chemical Co. (St. Louis, MO).

Pulse protocols and analysis. The holding potential was −80 mV unless otherwise indicated. After control data were obtained, bath perfusion was switched to drug-containing solution. The effects of drug infusion or removal were monitored as described in Results. The cycle time for protocols was 15 sec, or slower to accommodate longer pulse durations. The standard protocol to obtain current-voltage relationships and activation curves consisted of 5000-msec pulses that were imposed in 10-mV increments between −80 and +60 mV. Further details are given in the text and figure legends. The steady state current-voltage relationships were obtained by measuring the current at the end of the 5000-msec depolarizations. Between −90 and −40 mV, only passive linear leak was observed during short (100 msec) depolarizations (activation kinetics of *HERG* were slow at <−20 mV, see Results); least-squares fits to these data were used for passive leak correction. At potentials positive to 0 mV, a small endogenous current was observed in control cells, which could easily be separated from the *HERG* currents (see Results). The effects of dofetilide were determined from both the time-dependent suppression of outward current and the reduction in peak tail currents. Rundown of the HERG current was limited to 4.5 ± 1.1% (eight experiments) in 15 min. Specific protocols to determine state and time dependence of block are indicated in Results.

The time course of activation, recovery from fast inactivation, tail current deactivation, and drug-induced kinetic changes were fitted with a sum of exponentials. The voltage dependence of activation was fit with a Boltzmann equation: $y = 1/[1 + \exp(-(E - E_h)/k)]$, where k is the slope factor and E_h is the voltage at which 50% of the channels are activated. The curve-fitting procedure used a nonlinear least-squares (Gauss-Newton) algorithm; results were displayed in linear and semilogarithmic format together with a plot of the residual deviations of the data from the fitted curve (difference plot). Goodness of the fit and the required number of exponential components were judged by comparing χ^2 values statistically (F test) and by inspecting for systematic nonrandom trends in the difference plot. Results are expressed as mean ± standard error. Analysis of variance with appropriate post hoc comparisons was used to compare the differences in mean values; $p < 0.05$ was considered significant.

Results

Biophysical properties of *HERG* expressed in human cells. Before addressing the methanesulfonanilide sensitivity, we needed to determine the basic properties of *HERG* expressed in this mammalian expression system. Fig. 1 shows currents in *HERG*-transfected HEK 293 cells, identified through the use of GFP fluorescence. The biophysical properties were determined with two complementary protocols, using a common −80 mV holding potential. In the first protocol (Fig. 1A), 5000-msec step depolarizations to potentials between −80 and +60 mV were used to determine channel activation kinetics and steady state current-voltage relations. In the second protocol (Fig. 1B), we studied channel deactivation and rectification by stepping to various voltages after first opening the channel with a 1000-msec prepulse to +40 mV. In untransfected or mock-transfected cells, we observed a small outward current at potentials positive to 0 mV (Fig. 1C). This current displayed fast activation and slow inactivation: mean currents at 0, 20, and 40 mV were 21 ± 4, 52 ± 11, and 85 ± 16 pA, respectively, at 1 sec and 17 ± 4, 35 ± 9, and 58 ± 12 pA, respectively, at 5 sec (10 experiments). Importantly, the endogenous tail currents at −40 mV were too small to measure (Fig. 1C). This current was visible as an initial current jump preceding the much slower activating *HERG* current in transfected cells and did not interfere with the measurement of the large *HERG* tail currents (500-900 pA).

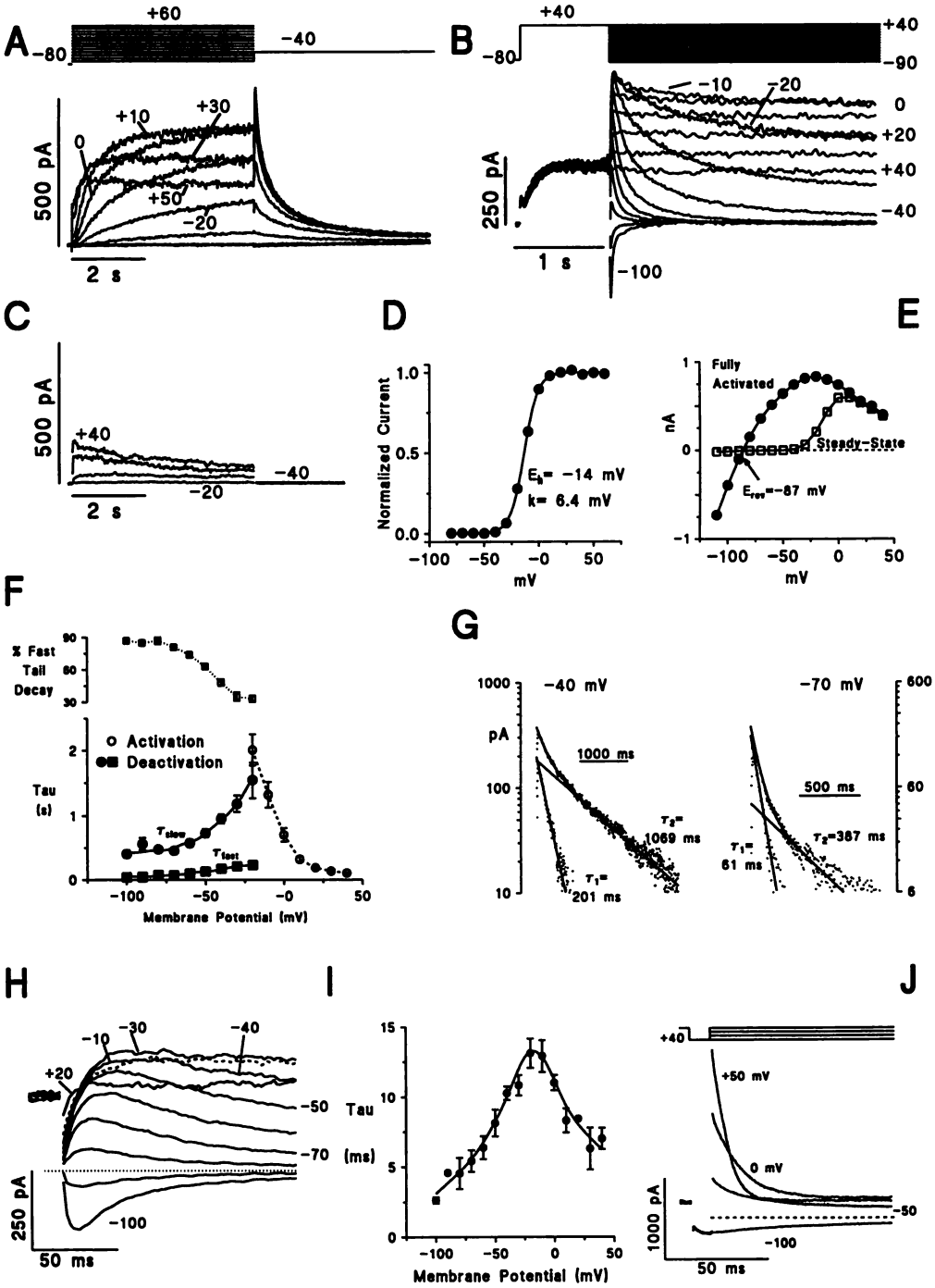

Fig. 1. Functional properties of *HERG* expressed in mammalian cells. A, Superimposed tracings evoked by depolarization to potentials between −70 and +50 mV. The rate of channel activation increased monotonically, but steady state current increased only up to +10 mV and declined with further depolarization. B, Inward rectification and deactivation of *HERG*. After fully activating the current with a fixed step to +40 mV, we measured currents at potentials between +40 and −100 mV. Between +40 and −10 mV, the outward current became progressively larger and remained steady. Negative to −10 mV, the tail currents declined with a rate that increased with hyperpolarization. C, Endogenous current in a mock-transfected HEK 293 cell. Pulse protocol as in A; tracings for steps to −20, 0, +20 and +40 mV. No tail currents are discernible at −40 mV; the outward current was <100 pA at +20 mV in this larger-than-average example (see text). D, Voltage dependence of activation determined from peak tail currents from experiments as in A. *Solid line*, fit with the Boltzmann distribution with the indicated parameters. E, Steady state and fully activated current-voltage relation. Both current-voltage relations demonstrate inward rectification of the outward current. The reversal potential for the fully activated current-voltage relation was −87 mV. The degree of rectification may be somewhat underestimated at positive potentials due to the presence of a small endogenous current. F, Kinetics of channel activation and deactivation. Activation was fit with a single exponential, but a double exponential was needed to describe tail current deactivation. The relative contribution of each component is indicated. G, Example of biexponential time course of tail current decay at −40 and −70 mV; at −70 mV, the fast component accounted for most of the decay. H, Initial rising phase of tail currents (pulse protocol as in B), illustrating that the rectification is not instantaneous. I, Voltage dependence of time constants of recovery from inactivation. Time constants were derived from monoexponential fits or represent the fast time constant of a biexponential fit for biphasic tail currents (i.e., negative to −50 mV). J, Triple-pulse paradigm demonstrating induction of inactivation. Pulse protocol as in B and H but with a 10-msec step to −100 mV preceding the second depolarization. Note the large currents at +50 mV.

In the experiment shown in Fig. 1A, no voltage-gated currents were observed with voltage steps between −80 and −50 mV. More positive depolarizations elicited a slowly increasing outward current that was followed by a pronounced deactivating tail current on repolarization to −40 mV. The rate of activation increased with progressive depolarization, but the size of the outward current reached a maximum at ~+10 mV. At more positive potentials, the amplitude of the current declined, so that at +60-70 mV, the small currents observed during depolarization were similar to those observed in untransfected cells. This behavior is consistent with the strong inward rectification observed for I_{Kr} in many mammalian cardiac myocytes and with the results for *HERG* expressed in oocytes as reported by Sanguinetti *et al.* (13). Despite the strong rectification during the depolarizing step, the deactivating tail currents at −40 mV remained large. They saturated at potentials of ≥10 mV and displayed a sigmoidal voltage dependence (Fig. 1D), which could be described with the use of a single Boltzmann distribution with a midpoint of −15.5 ± 1.7 mV (10 experiments) and a slope factor of 7.2 ± 0.3 mV. The rectification properties were further analyzed by measuring deactivating tail currents between −120 and +40 mV using the second protocol (Fig. 1B). Between +30 mV and −10 mV, the currents displayed a fast rising phase that settled into a substantially larger amount of steady outward currents compared with the current at +40 mV. This not only illustrates directly the inward rectification but also indicates that the rectification is not instantaneous. The *HERG* tail currents reversed between −80 and −90 mV (Fig. 1, B and E); the reversal potential was −85.2 ± 0.6 mV (nine experiments) with 4 mM external K^+, which is consistent with high K^+ selectivity.

The time course of activation could be fit with a single exponential, yielding time constants of 2008 ± 240 msec at −20 mV and 188 ± 21 msec at +20 mV (seven experiments). Fig. 1F shows the strong voltage dependence of the activation kinetics between −20 and +40 mV. At −40 mV, the activation time constant was 4.1 ± 0.9 sec (four experiments, fit to 10-sec depolarizing step). These slow activation kinetics may in part explain why no outward *HERG* current was observed by Trudeau *et al.* (14): they used primarily 250-msec voltage steps, which would activate little current below 0 mV. The time course of tail currents was more complex (Fig. 1, F and G). At least two exponential components were needed to describe the deactivation phase at −40 mV, with values of 214 ± 18 and 1407 ± 153 msec (nine experiments), respectively. Fig. 1G illustrates that the contribution of both components was approximately equal at −40 mV but that the faster component predominated at −70 mV. Fig. 1F summarizes the voltage dependence of both time constants and illustrates that the fractional contribution of the fast component increased with hyperpolarization. Taking advantage of the small capacitance of these mammalian cells, we analyzed the initial rising phase of the tail current in more detail. Fig. 1H shows that a time-dependent component was readily detected over the entire voltage range between −120 and +20 mV under physiological K^+ gradients. This phenomenon is consistent with time-dependent recovery from fast inactivation underlying the inward rectification, as originally proposed for I_{Kr} by Shibasaki (1). The time constant for this process was 9.9 ± 0.4 msec (10 experiments) at −40 mV, and the bell-shaped voltage dependence of this process is shown in Fig. 1I. A triple-pulse paradigm expanding on the observations in Fig. 1H was used to further determine the inactivation kinetics at positive potentials (Fig. 1J). After allowing a 10-msec recovery at −100 mV, the cell was depolarized again to positive potentials, revealing large outward currents (2-4 nA) that declined with a time constant of 6 ± 1 msec (four experiments) at +50 mV, which is consistent with the concept that rectification in this channel is due to fast inactivation.

Dofetilide block requires channel activation. We next investigated whether *HERG* expressed in mammalian cells displays the nanomolar methanesulfonanilide sensitivity that is typical of the cardiac delayed rectifier current, I_{Kr}. When we imposed a holding potential of −80 mV (Fig. 2A) to keep the channel in the closed conformation during wash-in of 30 nM dofetilide, the first depolarization after 10-15 min at −80 mV yielded little or no reduction in current (<10%, four experiments). Subsequently, block developed on a pulse-by-pulse basis, requiring an additional 10 min to achieve steady state (Fig. 2A). However, if the cells were held at −50 mV or −40 mV (i.e., around the threshold for opening), then extensive block was already apparent on the first depolarization after a 10-min equilibration period; the block further increased during subsequent depolarizations. The superposition of these tracings, as in Fig. 2B, suggests a possible mechanism for block. After a 12-min wash-in period in this example, the first tracing for 30 nM dofetilide showed little initial depression of the *HERG* current, which then slowly declined during the 30-sec depolarization, followed by a reduced tail current. The next pulse (45 sec later) started at the level of block at the end of the previous step, and this process was repeated with each subsequent depolarization (*horizontal dotted lines*). Thus, block developed slowly during the depolarization but not during the interpulse interval at −80 mV. A monoexponential fit to the declining peak tail current yielded a time constant of 221 sec (Fig. 2B, *inset*). When only time spent at depolarized potentials was considered, the time constant was 164 sec. Either way, this indicated that 30 nM dofetilide induced substantial block but that the onset of block was slow, with little recovery occurring between depolarizations.

The concentration dependence of block was therefore determined after sufficient equilibration promoted through a combination of step depolarizations and, for 10 nM dofetilide, a holding potential of −50 to −40 mV. The concentration dependence of block derived from suppression of tail currents at −40 mV revealed an apparent affinity of 12 ± 2 nM (Fig. 2C) (pooled data from 15 experiments with one or more dofetilide concentrations tested). After obtaining steady state conditions, we tested for superimposed use-dependent block. However, with pulse trains at frequencies of 1-0.2 Hz (500- or 2000-msec steps to +20 mV from a holding potential of −80 mV), we did not observe significant changes in the level of block (10 or 30 nM). A comparison of the amplitude of the tail currents between +10 and +60 mV (where channel activation saturated; Fig. 1D) did not reveal a superimposed intrinsic voltage dependence of block.

These results suggested that channel activation was required for the slowly developing block. Fig. 3 shows the result of an experiment to directly test this hypothesis. This cell was held at −80 mV for 10 min during exposure to 300 nM dofetilide (30-fold above the EC_{50}). During the first depolar-

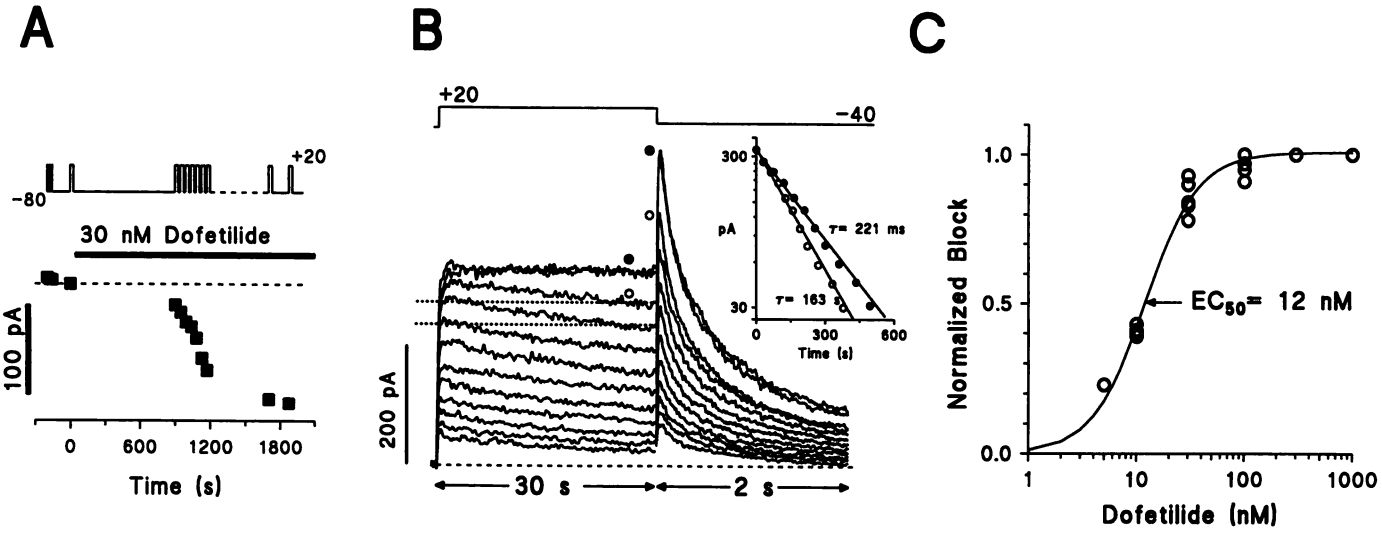

Fig. 2. Dofetilide block of *HERG*. A, Pulse-dependent development of block with 30 nM dofetilide. ■, Size of the tail current evoked by voltage steps to +20 mV. After switching to 30 nM dofetilide, we held the cell at −80 mV for 900 sec. A series of steps (20 sec at +20 mV, 2 sec at −40 mV) were then applied at 45-sec intervals. The last two points were obtained after steps to other voltages had been applied (*dashed line*, interval). B, Kinetics of block development during depolarization. Note the difference in time scale for the step and tail segment. The pulse sequence was as in A. The two superimposed control steps (●) were separated by a 12-min interval from the first step in drug (○). The subsequent interval was 45 sec, except for the *bottom two tracings* (60 sec). *Horizontal dotted lines*, subsequent pulses started at the level of block established at the end of the previous step. The time course of the tail currents was not markedly altered. *Inset*, exponential fit to decline of current against real time (●) or depolarized time only (○). C, Concentration dependence of *HERG* block by dofetilide. Suppression of peak tail current at −40 mV (four to six experiments at each concentration). *Solid line*, least-squares fit to the data with the Hill equation $f = 1/[1 + (EC_{50}/D)^n]$, where f is fractional block, [D] is dofetilide concentration, EC_{50} is the concentration for 50% block, and n is the Hill coefficient (n = 1.7).

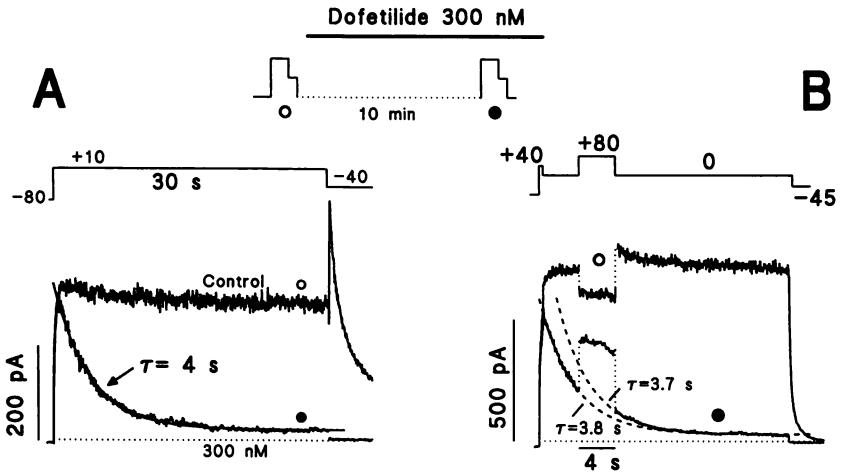

Fig. 3. Time-dependent block during a depolarization with 300 nM dofetilide. A, After the control tracing was obtained, the cell was held at −80 mV for 10 min while dofetilide was allowed to equilibrate (*inset*). During the first step in the presence of dofetilide, the *HERG* current activated initially as in control. The exponential fit to the subsequent decline is superimposed on the tracing (*solid line*). Note that the tail current was completely suppressed. B, Delay in block development by depolarization to +80 mV. A 400-msec prepulse to +40 mV preceding the sustained depolarization to 0 mV was used to speed up channel opening. After 4 sec, a step to +80 mV was superimposed, which reduced the control current, reflecting strong rectification. Exponential fits with the indicated time constants are superimposed on the tracing in the presence of dofetilide and illustrate the 1.9-sec delay in block development induced by the depolarization to +80 mV.

ization in the presence of dofetilide, the current initially activated as in control but subsequently displayed a time-dependent decline with a time constant of 4 sec. With this paradigm, the time constant for onset of block averaged 5.2 ± 0.6 sec (five experiments) for 300 nM dofetilide. The complete suppression of the subsequent tail currents (five experiments) confirmed that all *HERG* current had been blocked during this single depolarization. In an additional experiment with 1000 nM dofetilide, the time-dependent block occurred faster [time constant τ = 1.1 sec]. To evaluate whether stronger depolarizations would enhance block, we superimposed a 4-sec depolarization to +80 mV on the step to +0 mV. Fig. 3B shows that the time-dependent decline of current at +0 mV in the presence of 300 nM dofetilide was interrupted by this strong depolarization but resumed its exponential time course when the potential was restored to +0 mV. This apparent delay of block development was quantified by the horizontal shift in the exponential fits (Fig. 3B). The average delay was 2.7 ± 0.6 sec (seven experiments) with the 4-sec intervening depolarization.

Open channel block may result in a modification of the time course of channel closure as has been observed for quinidine and other open channel blockers (20, 21). Therefore, we determined the kinetics of channel deactivation and of fast recovery from inactivation. Neither 10 nor 30 nM dofetilide (which induce 30-80% block) had significant effects on the time course of the tail currents. Deactivation time constants at −40 mV were 183 ± 21 and 1295 ± 144 msec, respectively (six experiments). Neither value was significantly different from the control values (see above). The bell-shaped voltage dependence of the time constant for recovery from fast inactivation was preserved (three experi-

ments), and at −40 mV, the time constant for recovery from fast inactivation was not significantly different from control (8.3 ± 0.7 versus 8.9 ± 0.9 msec, five experiments; p = NS, paired comparison).

Discussion

This study represents, to the best of our knowledge, the first report on the properties of *HERG* currents expressed in human cells studied under ionic conditions similar to those used in the study of cardiac myocytes. The main findings are that mammalian expression of *HERG* resulted in a K^+-selective outward current that was sensitive to the methanesulfonanilide dofetilide. Activation and deactivation kinetics were slow at potentials negative to 0 mV. The current displayed inward rectification at positive potentials, resulting in large tail currents on repolarization to −40 mV. Block of *HERG* by dofetilide required channel activation and resulted in time-dependent decline of the open channel current. These properties are very similar to those of I_{Kr} in myocytes (1-4) and resemble the currents described in *Xenopus* oocytes by Sanguinetti *et al.* (13). Detailed analysis of the induction of fast inactivation was beyond the scope of this study and remains to be demonstrated in the native preparations.

Methanesulfonanilide sensitivity is essentially the pharmacological definition of I_{Kr} because this group of class III drugs is highly selective for this channel (8). Our results demonstrate that *HERG* shares this property, despite the initial suggestion that an additional subunit might be needed to confer the proper pharmacology (13). The EC_{50} observed under our experimental conditions is similar to the EC_{50} reported for I_{Kr} in mouse AT-1 cells (12 nM) (6), rabbit ventricular myocytes (4 nM) (7), and guinea pig myocytes (31 nM) (8). The results are also consistent with radioligand binding studies that indicate high affinity sites with values of 47 nM (22) or 28 nM (23). The *HERG* channel is much more sensitive to dofetilide than the traditional inward rectifier hIRK (EC_{50} = 533 nM) (24), which further underscores the high selectivity of this methanesulfonanilide drug.

The mechanism of I_{Kr} block by dofetilide has not been firmly established, although the requirement of channel activation for block and use-dependent unblock during washout suggest open channel block (6-8). In cell-attached configuration, I_{Kr} single channels are blocked by E4031 applied to the bath, indicating that methanesulfonanilide block occurs from the cytoplasmic side (25). The results illustrated in Figs. 2 and 3 provide direct evidence for open (or activated-state) channel block: 1) the observation that block was prevented when the channels were kept in their closed conformation while the drug equilibrated in the cell argues against closed state block, and 2) the delay in block induced by stronger depolarizations (Fig. 3B) indicates a low affinity of the inactivated state as well. At low concentrations, block subsequently developed in a pulse-dependent manner, but long depolarizations were required. To directly demonstrate time-dependent block during a single depolarization, we needed concentrations that were ≥~30-fold the EC_{50} (Fig. 3). The limited amount of block during the first step at concentrations approximating the EC_{50} may explain why high affinity methanesulfonanilide block of *HERG* was not observed in previous studies (13, 14).

The time constant of block development with 300 nM dofetilide allows an estimate of apparent binding and dissociation rate constants. Assuming a bimolecular reaction, the rate of block $\lambda = 1/\tau_{block} = k*[D] + l$ or $\lambda \approx k*[D]$ at this saturating concentration. From the 5.2-sec time constant, we obtain λ = 0.19 sec^{-1} and k = 0.6 μM^{-1} sec^{-1}, and an apparent dissociation rate constant l = 0.007 sec^{-1} (calculated from $EC_{50} = l/k$). The latter is in reasonable agreement with the dissociation rate constant (0.0026 sec^{-1}) obtained from radioligand binding studies (23, 26), which also showed slow time constants for association (255 and 348 sec for 10 and 12 nM dofetilide, respectively). The slow interaction kinetics are also consistent with the lack of steady state use dependence in action potential prolongation or I_{Kr} block observed with this drug (7, 8). Open channel blockers may slow channel deactivation, resulting in a "cross-over" phenomenon with the current in control, an effect observed for block of hKv1.5 by quinidine and several other drugs (20, 21). We did not detect such an effect for the interaction of dofetilide with expressed *HERG* currents. However, because this drug-induced modification of deactivation kinetics depends critically on the relative rates for channel deactivation and drug/channel interaction, this result is not an argument against an open (or activated) channel block mechanism. The estimate for the dissociation rate constant for dofetilide indicates a dissociation time constant of 1/0.007 = 142 sec, which would be too slow to induce observable changes in deactivation time course. An alternate mechanism is that dofetilide would bind to the fast inactivated state that underlies the rectification. This is unlikely because no changes in tail current kinetics were observed after depolarizations between +10 and +60 mV and because strong depolarizations delayed block development, rather than enhancing it.

Nevertheless, this fast inactivation process (Fig. 1, H–J) puts an additional constraint on the interpretation of the drug/channel interaction. If 90% of the channels rectify at ~+10 mV due to this dynamic process (1, 13), an open channel receptor would be available only 10% of the time. Because of the fast rates involved (Fig. 1, H and I; 70-300 sec^{-1}), this inactivation process would compete with drug binding and therefore slow drug association, which is similar to interactions of tetraethylammonium with N-type inactivation or to slowing of tetrapentylammonium block of hKv1.5 by quinine (21, 27). We tested the potential impact on the observable the time course of open channel block using mathematical simulations comparing conditions of low, intermediate, and high levels of fast inactivation (Fig. 4). Condition *c* would correspond to the level of fast inactivation observed for *HERG*. As the degree of fast inactivation is increased (compare *a* with *c*), the observable rate of drug binding declines considerably. If dofetilide can only bind to the open conformation, the apparent association rate constant mentioned above would correspond to a microscopic rate constant of ~5 μM^{-1} sec^{-1}. This value is more consistent with typical values for organic open channel blockers (3-15 μM^{-1} sec^{-1}) than with the k = 0.6 μM^{-1} sec^{-1} value estimated without this consideration. Therefore, the unique feature of this channel, fast but reversible inactivation on a time scale much faster than channel opening, needs to be considered when interpreting open channel block mechanistically. In principle, a better estimate would be obtained at lower voltages, where rapid inactivation is less extensive, but the slow channel kinetics at <−20 mV preclude such an approach.

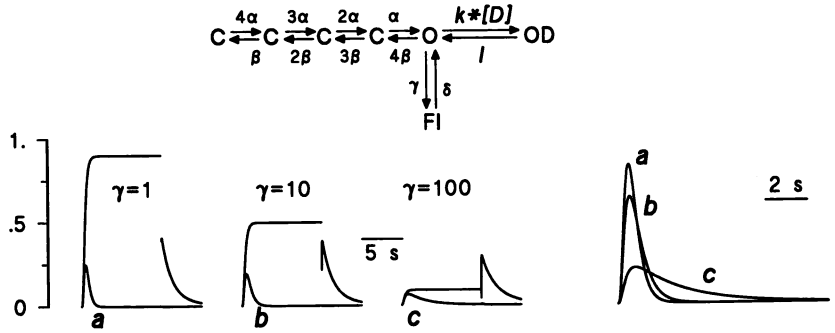

Fig. 4. Simulation of the impact of inactivation on observable kinetics of block. Model and mathematical techniques are similar to the model used to interpret drug block of hKv1.5 (20, 21) but with activation rates adjusted for the slower kinetics of *HERG*: $\alpha = 4\ sec^{-1}$ and $\beta = 0.01\ sec^{-1}$ at +20 mV and $\alpha = 0.08\ sec^{-1}$ and $\beta = 0.2\ sec^{-1}$ at −40 mV. *C*, Closed states; *O*, open state; *FI*, fast inactivated state; *OD*; dofetilide-blocked open state. Fast inactivation modeled with $\gamma = 100\ sec^{-1}$ and $\delta = 10\ sec^{-1}$ resulted in ~90% inactivation (with $\tau = 9$ msec). Recovery from fast inactivation at −40 mV was reproduced with $\gamma = 20\ sec^{-1}$ and $\delta = 50\ sec^{-1}$. Drug association and dissociation rate constants were $k = 5\ \mu M^{-1}\ sec^{-1}$ and $l = 0.005\ sec^{-1}$, with [D] = 1 μM. For simulations a–c, all model rate constants were kept identical, except that inactivation was reduced by lowering γ (10 or 1 sec^{-1}). *Right*, superimposed tracings in drug from the simulations a–c. Despite the identical rate constants for the drug/channel interaction, the apparent rate of drug block was slowed from 3 sec^{-1} (a) to 2 sec^{-1} (b) and 0.4 sec^{-1} (c) as the degree of fast inactivation was increased.

In conclusion, *HERG* currents observed after expression in HEK 293 cells displayed both biophysical and pharmacological properties of I_{Kr}. The results indicate that there is no compelling reason to invoke ancillary subunits to account for high affinity methanesulfonanilide block. Dofetilide was found to be a slow-onset/slow-offset open channel blocker, and the unique gating properties of this channel pose interesting challenges to the interpretation of drug/channel interactions. Finally, demonstration that *HERG* displays the proper methanesulfonanilide sensitivity further strengthens the mechanistic link between hereditary and acquired forms of the LQTS.

Acknowledgments

We thank Dr. Gail Robertson for providing the mammalian *HERG* expression construct; Drs. Dan Roden, Michael Tamkun, and Paul Bennett for their critical review of the manuscript; and Tom Rich and Sarita Yeola for technical assistance.

References

1. Shibasaki, T. Conductance and kinetics of delayed rectifier potassium channels in nodal cells of the rabbit heart. *J. Physiol. (Lond.)* **387**:227-250 (1987).
2. Sanguinetti, M. C., and N. K. Jurkiewicz. Two components of cardiac delayed rectifier K^+ current: differential sensitivity to block by class III antiarrhythmic agents. *J. Gen. Physiol.* **96**:195-215 (1990).
3. Balser, J. R., P. B. Bennett, and D. M. Roden. Time-dependent outward current in guinea pig ventricular myocytes: gating kinetics of the delayed rectifier. *J. Gen. Physiol.* **96**:835-863 (1990).
4. Yang, T., M. S. Wathen, A. Felipe, M. M. Tamkun, D. J. Snyders, and D. M. Roden. K^+ currents and K^+ channel mRNA in cultured atrial cardiac myocytes (AT-1 cells). *Circ. Res.* **75**:870-878 (1994).
5. Follmer, C. H., and T. J. Colatsky. Block of delayed rectifier potassium current, I_K, by flecainide and E4031 in cat ventricular myocytes. *Circulation* **82**:289-293 (1990).
6. Yang, T., D. J. Snyders, and D. M. Roden. Ibutilide, a methanesulfonanilide antiarrhythmic, is a potent blocker of the rapidly activating delayed rectifier K^+ current (I_{Kr}) in AT-1 cells: concentration-, time-, voltage-, and use-dependent effects. *Circulation* **91**:1799-1806 (1995).
7. Carmeliet, E. Voltage- and time-dependent block of the delayed K^+ current in cardiac myocytes by dofetilide. *J. Pharmacol. Exp. Ther.* **262**:809-817 (1992).
8. Jurkiewicz, N. K., and M. C. Sanguinetti. Rate-dependent prolongation of cardiac action potentials by a methanesulfonanilide class III antiarrhythmic agent: specific block of rapidly activating delayed rectifier K^+ current by dofetilide. *Circ. Res.* **72**:75-83 (1993).
9. Colatsky, T. J., and T. M. Argentieri. Potassium channel blockers as antiarrhythmic drugs. *Drug Dev. Res.* **33**:235-249 (1994).
10. Roden, D. M. Current status of class III antiarrhythmic drug therapy. *Am. J. Cardiol.* **72**:44B–49B (1993).
11. Warmke, J. W., and B. Ganetzky. A family of potassium channel genes related to *eag* in *Drosophila* and mammals. *Proc. Natl. Acad. Sci. USA* **91**:3438-3442 (1994).
12. Curran, M. E., I. Splawski, K. W. Timothy, G. M. Vincent, E. D. Green, and M. T. Keating. A molecular basis for cardiac arrhythmia: HERG mutations cause long QT syndrome. *Cell* **80**:795-803 (1995).
13. Sanguinetti, M. C., C. Jiang, M. E. Curran, and M. T. Keating. A mechanistic link between an inherited and an acquired cardiac arrhythmia: HERG encodes the I_{Kr} potassium channel. *Cell* **81**:299-307 (1995).
14. Trudeau, M. C., J. W. Warmke, B. Ganetzky, and G. A. Robertson. HERG, a human inward rectifier in the voltage-gated potassium channel family. *Science (Washington D. C.)* **269**:92-95 (1995).
15. Wang, Z., B. Fermini, and S. Nattel. Rapid and slow components of delayed rectifier current in human atrial myocytes. *Cardiovasc. Res.* **28**:1540-1546 (1994).
16. Ohler, A., G. J. Amos, E. Wettwer, and U. Ravens. Frequency-dependent effects of E-4031, almokalant, dofetilide and tedisamil on action potential duration: no evidence for "reverse use dependent" block. *Naunyn-Schmiedeberg's Arch. Pharmacol.* **349**:602-610 (1994).
17. Chadwick, C. C., D. S. Krafte, B. O'Connor, W. A. Volberg, A. M. Ezrin, R. E. Johnson, and P. J. Silver. Evidence for multiple antiarrhythmic binding sites on the cardiac rapidly activating delayed rectifier K^+ channel. *Drug Dev. Res.* **34**:376-380 (1995).
18. Chalfie, M., Y. Tu, G. Euskirchen, W. W. Ward, and D. C. Prasher. Green fluorescent protein as a marker for gene expression. *Science (Washington D. C.)* **263**:802-805 (1994).
19. Hamill, O. P., A. Marty, E. Neher, B. Sakmann, and F. J. Sigworth. Improved patch clamp techniques for high-resolution current recording from cells and cell-free membrane patches. *Pfluegers Arch. Eur. J. Physiol.* **391**:85-100 (1981).
20. Snyders, D. J., K. M. Knoth, S. L. Roberds, and M. M. Tamkun. Time-, voltage-, and state-dependent block by quinidine of a cloned human cardiac potassium channel. *Mol. Pharmacol.* **41**:322-330 (1992).
21. Snyders, D. J., and S. W. Yeola. Determinants of antiarrhythmic drug action: electrostatic and hydrophobic components of block of the human cardiac hKv1.5 channel. *Circ. Res.* **77**:575-583 (1995).
22. Lynch, J. J., Jr., E. P. Baskin, E. M. Nutt, P. J. Guinosso, Jr., T. Hamill, J. J. Salata, and C. M. Woods. Comparison of binding to rapidly activating delayed rectifier K^+ channel, I_{Kr}, and effects on myocardial refractoriness for class III antiarrhythmic agents. *J. Cardiovasc. Pharmacol.* **25**:336-340 (1995).
23. Duff, H. J., Z. Feng, and R. S. Sheldon. High- and low-affinity sites for [^{3}H]dofetilide binding to guinea pig myocytes. *Circ. Res.* **77**:718-725 (1995).
24. Kiehn, J., B. Wible, E. Ficker, M. Taglialatela, and A. M. Brown. Cloned human inward rectifier K^+ channel as a target for class III methanesulfonanilides. *Circ. Res.* **77**:1151-1155 (1995).
25. Veldkamp, M. W., A. C. van Ginneken, and L. N. Bouman. Single delayed rectifier channels in the membrane of rabbit ventricular myocytes. *Circ. Res.* **72**:865-878 (1993).
26. Chadwick, C. C., A. M. Ezrin, B. O'Connor, W. A. Volberg, D. I. Smith, K. J. Wedge, R. J. Hill, G. M. Briggs, E. D. Pagani, P. J. Silver, and D.S. Krafte. Identification of a specific radioligand for the cardiac rapidly activating delayed rectifier K^+ channel. *Circ. Res.* **72**:707-714 (1993).
27. Choi, K. L., R. W. Aldrich, and G. Yellen. Tetraethylammonium blockade distinguishes two inactivation mechanisms in voltage-activated K^+ channels. *Proc. Natl. Acad. Sci. USA* **88**:5092-5095 (1991).

Send reprint requests to: Dirk J. Snyders, M.D., Departments of Medicine and Pharmacology, 554-MRB2, Vanderbilt University School of Medicine, Nashville, TN 37232-6602, E-mail: dirk.snyders@mcmail.vanderbilt.edu